Titel/Title: Modeling of Surface Generation in Contour Grinding of Optical Molds

Autor*innen/Author(s): C. Heinzel, D. Grimme, A. Moisan

Veröffentlichungsversion/Published version: Postprint

Publikationsform/Type of publication: Artikel/Aufsatz

Empfohlene Zitierung/Recommended citation:

C. Heinzel, D. Grimme, A. Moisan: Modeling of Surface Generation in Contour Grinding of Optical Molds. CIRP Annals, Volume 55, Issue 1, 2006, Pages 581-584
ISSN 0007-8506, https://doi.org/10.1016/S0007-8506(07)60487-9.
(https://www.sciencedirect.com/science/article/pii/S0007850607604879)

Verfügbar unter/Available at:
(wenn vorhanden, bitte den DOI angeben/please provide the DOI if available)

10.1016/S0007-8506(07)60487-9

Zusätzliche Informationen/Additional information:

Modeling of Surface Generation in Contour Grinding of Optical Molds

C. Heinzel[1], D. Grimme[1]
[1]Laboratory for Precision Machining
University of Bremen, Germany
Submitted by A. Moisan (1), ENSAM, Cluny, France

Abstract
The objective of this paper is the modeling of kinematics of precision contour grinding and resulting workpiece topography. Changes within the contact zone of grinding wheel and workpiece as well as speed ratios are analyzed and evaluated. The generated surface patterns caused by the runout of the grinding wheel are simulated. In the kinematic-geometrical model single grains on the peripheral surface of a grinding wheel, which interact with the workpiece, are considered. After describing the kinematics of the contour grinding process, changes in feed speeds and rotational speed ratios are examined and their effects on generated surfaces are simulated and compared with ground surfaces.

Keywords:
Modeling, Surface, Grinding

1 INTRODUCTION

The research on grinding operations and resulting surface roughness has provided several kinematic, kinematic-analytical and kinematic-geometrical models. 3D kinematic-geometrical models became possible by advanced high capacity computer systems. Such models were developed and applied not only to gain a better understanding but also to optimize grinding processes [1, 2, 3]. Most of the models are assuming ideally stiff grinding processes, whereas in [4] the elastic deflection of grains as well as the plastic material behaviour are also considered. Although the above mentioned models provide information on surface roughness and chip formation, they do not describe recurrent surface discontinuities of ultra precision ground surfaces. Ultra precision grinding is used to generate complex molds and lenses for optical applications. The aim of the ultra precision contour grinding process is to generate high surface quality and integrity as well as high form accuracy to reduce the effort in the necessary subsequent polishing process. But although ultra precision machine tools are applied and peak to valley figure errors of less than 0.5 µm as well as surface roughness less than 10 nm Rq can be achieved, small surface discontinuities can be observed frequently. These surface quality degradations can be associated with self induced vibrations that may occur during grinding [5, 6, 7]. However, also irregular and instationary process conditions in grinding (e.g. wheel runout) may lead to unfavourable formation of surface patterns and consequently to inferior component quality [8].

This paper presents an investigation of contour grinding kinematics, geometry, and the generation of unintended surface patterns. Besides of chatter these surface patterns originate from various causes. They are influenced by the kinematics of the machining process as well as by e.g. wheel runout, machine vibrations, workpiece inhomogeneities and unbalanced tools [9, 10]. The presented model is developed for precision contour grinding and was designed to run with regular computer power. The algorithm was composed to describe occurring surface patterns on the ground workpiece surface. Different to most of the known models it does not model the micro topography, which is generated by the wheel topography. The presented model deals with the interaction of grinding wheel and workpiece and explains the origin of occurring surface discontinuities. This knowledge will help to improve grinding processes before machining and to decrease subsequent polishing time.

2 CONTOUR GRINDING GEOMETRY AND KINEMATICS

The kinematics of the contour grinding process can be described by two superimposed rotational motions of the grinding wheel and the workpiece, as well as at least one linear motion of either the grinding wheel or the workpiece, see Figure 1.

Material removal by grinding can be described by the superimposed engagement of single cutting points. Unlike polishing processes the bonded grains in grinding are moving on a defined path, predetermined by the relative motion of the workpiece and grinding wheel.

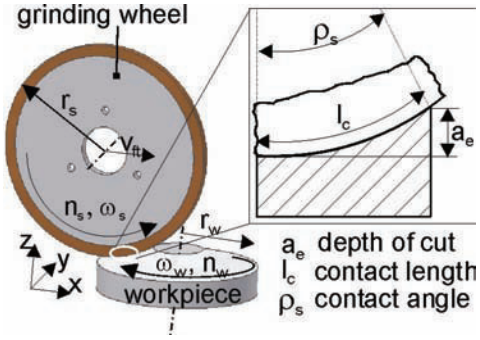

Figure 1: Schematic of the contour grinding geometry and kinematics.

2.1 Grinding results and motivation for the work

In contour grinding experiments on PVD-TiNiN-coated and hardened steel specimens applying an ultra precision machine tool, recurrent surface discontinuities in form of spirals and even more complex patterns were observed, see Figure 2. The flat steel specimen (a) was ground with a vitreous bonded grinding wheel having 10-20 µm cBN grits. Grinding parameters within the typical settings for precision grinding were applied. A 10 µm depth of cut a_e, a feed speed v_{ft} of 3 mm/min, a peripheral wheel speed v_s of 25 m/s and a rotational speed n_w of 250 rpm for the workpieces were applied.

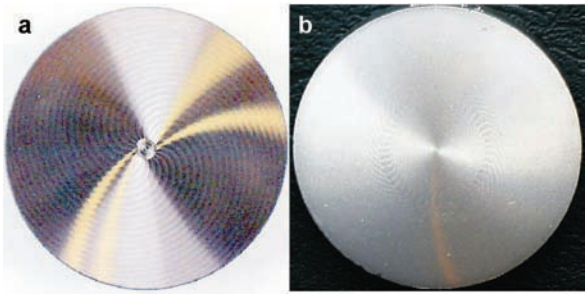

Figure 2: Surface patterns on face (a) and a spherical (b) ground specimens.

The spherical PVD-coated specimen (b) was ground with a resin bonded diamond wheel with a grit size of 3 µm, a feed speed v_{ft} of 2 mm/min, a 3 µm depth of cut a_e, a wheel speed v_s of 25 m/s and a workpiece rotational speed n_w of 250 rpm. Even when using a soft resinoid bonded diamond wheel with a high damping factor surface discontinuities remained detectable, the origin of which will be analyzed and modeled in the following.

2.2 Modeling

During contour grinding each single cutting edge around the wheel periphery moves on a three dimensional path through the workpiece material forming chips. If the grinding parameters as well as the geometrical factors are quantitatively known, it is possible to describe the spatiotemporal motion of a single grain cutting edge mathematically. The kinematic path of one single grain (P) through the material in contour grinding can be calculated by integrating the effective cutting speed $v_{c.eff}$.

$$\mathbf{v}_{c.eff} = \left(v_x, v_y, v_z\right) \tag{1}$$

The effective cutting speed results from the relative motion between grain and workpiece and can be decomposed into the three components v_x, v_y and v_z, see the following equations:

$$v_x = r_s \cdot \omega_s \cdot cos\left(\theta_s\right) - r_{wp} \cdot \omega_w \cdot cos\left(\theta_w\right) + v_{ft} \tag{2}$$

$$v_y = r_{wp} \cdot \omega_w \cdot sin\left(\theta_w\right) \tag{3}$$

$$v_z = r_s \cdot \omega_s \cdot sin\left(\theta_s\right), \tag{4}$$

where r_{wp} is the radius of the current position of the grain interacting with the workpiece, r_s the radius of the grinding wheel, ω_s the angular velocity of the grinding wheel and ω_w the angular velocity of the workpiece.

For the modeling of the cutting paths of the grains over the component surface, three frames of reference were used, one for the workpiece x', y', z', one for the grinding tool x'', y'', z'' and one fixed coordinate system x, y, z, see Figure 4.

Both frames of reference, workpiece and fixed frame, originate from the rotational center of the workpiece. The origin of the tool reference frame is located within the center of the grinding wheel and its x axis is moving with the feed speed of either the grinding wheel or the workpiece.

Applying a coordinate transformation the tool coordinate system x''-y''-z'' can be transformed into the fixed frame x-y-z. The superposition of the rotational and tangential motion of the grinding wheel leads to the equations (5)-(7).

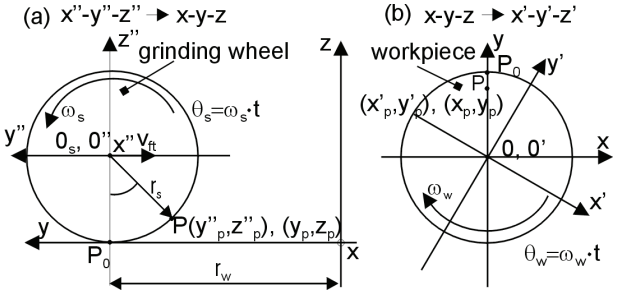

Figure 4: Definition of coordinate systems.

$$x_p = x''_p + x_{0''} = 0 \tag{5}$$

$$y_p = y''_p + y_{0''} = r_w - r_s \cdot sin\left(\omega_s \cdot t\right) - v_{ft} \cdot t \tag{6}$$

$$z_p = r_s - r_s \cdot \cos\left(\omega_s \cdot t\right) \tag{7}$$

Since the effective cutting process results from the relative motion between workpiece and grinding wheel, a coordinate transformation of the fixed frame x-y-z into the x'-y'-z' system is required, which rotates around the z axis of the workpiece with ω_w.

$$\begin{aligned} x'_p &= x_p \cdot cos\left(\omega_w \cdot t\right) - y_p \cdot sin\left(\omega_w \cdot t\right) \\ &= sin\left(\omega_w \cdot t\right) \cdot \left[r_s \cdot sin\left(\omega_s \cdot t\right) + v_{ft} \cdot t - r_w\right] \end{aligned} \tag{8}$$

$$\begin{aligned} y'_p &= x_p \cdot sin\left(\omega_w \cdot t\right) + y_p \cdot cos\left(\omega_w \cdot t\right) \\ &= cos\left(\omega_w \cdot t\right) \cdot \left[r_w - r_s \cdot sin\left(\omega_s \cdot t\right) - v_{ft} \cdot t\right] \end{aligned} \tag{9}$$

$$z'_p = z_p = r_s - r_s \cdot cos\left(\omega_s \cdot t\right) \tag{10}$$

By applying these equations it is possible to describe each current position of one point of the grinding wheel periphery on the workpiece surface and its locus change during the process. Since the cutting edges on the periphery of the grinding wheel do interact only a short time the periodic interaction T of a cutting edge with the workpiece results from the constant angular speed and the contact angle ρ_s to

$$T = \frac{\rho_s}{\omega_s} = \frac{arccos\left(1 - a_e / 2r_s\right)}{2\pi \cdot n_s}, \tag{11}$$

where a_e is the depth of cut, n_s the rotational speed of the grinding wheel and r_s the grinding wheel radius.

By describing the grain/workpiece interaction from the beginning of engagement $t = t_{in}$

$$t_{in} = \left(\frac{n}{n_s}\right) \quad n = 0, 1, .., N$$

until the end of engagement $t = t_{out} = t_{in} + T$

as well as any time of grain/workpiece interaction in-between, the visualization of the 3D grain path through the workpiece becomes possible. In the following the deepest points of interaction are considered.

2.3 Simulation results

The mathematical description of the grinding process kinematics and geometry are preconditions to model the grinding process and to visualize in particular the grain paths on the surface of the workpiece. To simplify matters it is assumed that one single grain on the grinding wheel periphery interacts with the workpiece at constant grinding parameters. The applied software tool, Matlab, which was applied to visualize the grain interaction with the

workpiece, takes into account only the maximum depth of cut and leaves a mark on the surface. During grinding the rotational frequency of the grinding wheel is determining the interaction frequency of the grain, the higher the rotational speed the higher the frequency and the more often the grain interacts with the workpiece. A variation of the rotational speed of the workpiece has also an influence on the grain/workpiece interaction, see Figure 5.

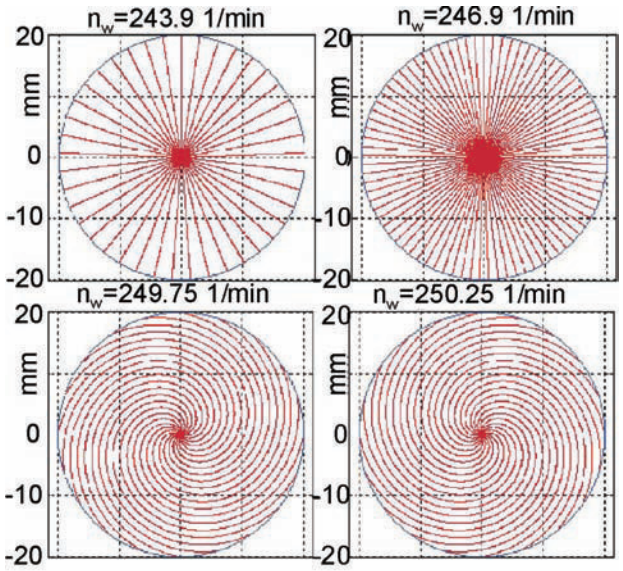

Figure 5: Simulated surfaces generated by single grain interaction increasing the rotational speed of the workpiece n_w.

Figure 5 depicts four simulated surface patterns generated by a single grain on the wheel periphery, increasing the rotational speed n_w of the workpiece. The speed ratio between grinding wheel and workpiece determines the number of contact points over the surface. In this example the wheel speed as well as the feed speed were kept constant at n_s = 5000 rpm and v_{ft} = 6 mm/min, respectively, and the speed of the workpiece n_w was slightly increased from 243.9 up to 250.25 rpm. The typical rotational speed of the workpiece in contour grinding experiments was adjusted to 250 rpm so that the simulated range reflects the speed range of the experiments. The patterns created on the surface are depending on the speed ratio between grinding wheel and workpiece. Increasing the rotational speed from 243.9 up to 250.25 rpm the depicted straight lines increase their density. If the speed ratio is decreasing further, the straight line pattern is changing into a spiral.

The modeling of the above shown grain interaction was based on the assumption that the grinding process is running without any malfunction like runout, eccentricity or velocity variations. But experimental results show that some small faults during the grinding process can not be avoided completely at any time. For this reason, irregularities in the grinding process were occurring from time to time causing surface discontinuities. That was the motivation to simulate malfunctioning grinding processes to gain an understanding of the arising surface patterns. Within the modeling approach of the grinding processes eccentricity, runout of the grinding wheel or different grain protrusion heights as well as rotational speed fluctuations during the grinding process were considered and the influence of these factors on the generation of ground surfaces was investigated. Therefore, also multiple grains uniformly distributed on the grinding wheel periphery were considered in a second approach. Additionally, a runout with the rotation frequency of the grinding wheel and a small amplitude in z-direction were taken into account. The coordinates of the deepest grain position were initially computed. The grain position height changes during the interaction caused by the modeled runout of the wheel and is depicted by different colours in Figure 6. The fluctuation in speed ratio between grinding wheel and workpiece is modeled by the change of the workpiece angular acceleration α. In this particular case, where the acceleration is changing continuously, it is possible to describe the position of one grain on the workpiece surface by the following equations (for the accelerated workpiece speed):

$$x'_p = \sin\left(\omega_w \cdot t + \frac{1}{2}\alpha \cdot t^2\right) \cdot \left(v_{ft} \cdot t - r_w\right) \qquad (11)$$

$$y'_p = \cos\left(\omega_w \cdot t + \frac{1}{2}\alpha \cdot t^2\right) \cdot \left(r_w - v_{ft} \cdot t\right) \qquad (12)$$

Figure 6 depicts a simulated surface discontinuity caused by eccentricity, runout of the grinding wheel or differences in grain protrusion heights and fluctuations in the workpiece rotational speed.

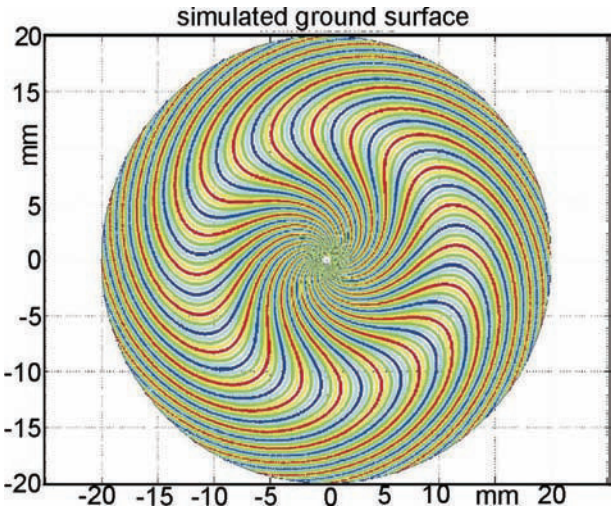

Figure 6: Simulated surface by applying eccentricity, wheel runout and fluctuations in the rotational workpiece speed.

The different coloured traces on the simulated surface are representing different depths of cut of the interacting grains.

2.4 Verification of simulated results

Besides the macroscopic modeling of surface discontinuities microscopic structures could also be simulated. Figure 7 depicts details of a ground surface measured with a white light interferometer, left, and the simulated surface, right. One measurement was performed near the center and one represents the ground center of the workpiece.

The ground surface exhibits a defined surface pattern. Darker regions alternate with lighter regions representing valleys and peaks in the measurements. It can also be seen that the different regions are overlapping. This is caused by spark out processes. Within the simulation result the different heights are depicted by different colours. Within the simulation of the workpiece center only the deepest depth of cuts are plotted so that the pattern becomes clearly visible.

As in face grinding with contour grinding kinematics, the mechanisms of generating surface discontinuities in form of patterns could also be applied to spherical grinding operations.

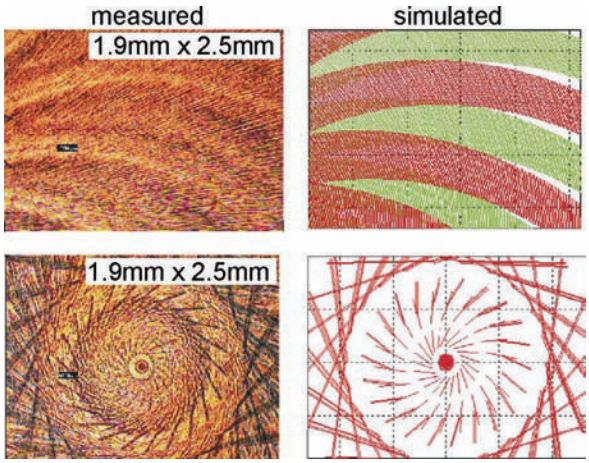

Figure 7: Measured and simulated microstructure of a face ground steel surface.

In comparison to the continuous patterns generated in face grinding, the patterns generated in spherical contour grinding differ in form, appearance and complexity. Also the number of the periodic structures on the spherical surface exceeds those on the face ground surface, although the grinding parameters are nearly the same. In order to gain an understanding of the reasons and the mechanisms of pattern formations, these surface structures were also studied, see Figure 8.

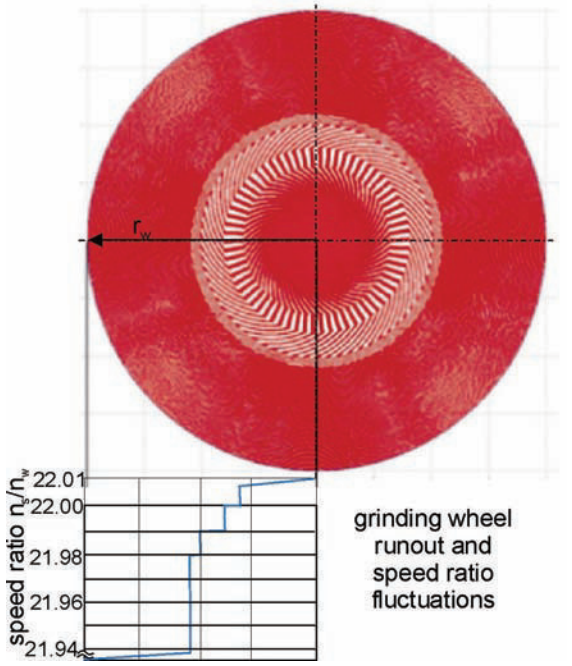

Figure 8: Simulated surface of a spherical workpiece, cf. Figure 2 b.

By varying the speed ratio as well as the runout of the grinding wheel, the real surface pattern was iteratively approximated. It could be shown by simulation of the ground surface that the grinding process was unsteady in this case. It was found that small but escalating changes in the speed ratio between workpiece and grinding wheel combined with a certain runout or differences in grain protrusion heights were responsible for the surface discontinuities on the real spherical workpiece.

3 CONCLUSIONS

In this paper the geometry and kinematics of the contour grinding process were analyzed and described. These analyses were applied to describe the grain/workpiece interaction in order to model the grinding process and resulting surface discontinuities which can be observed from time to time in ultra precision grinding experiments. To gain the knowledge of the origin of these discontinuities the model was applied to the generation of ground surfaces. By varying speed ratios, feed speeds and runout errors, the model was used to simulate the generation of surface patterns. It was shown that the results of the simulation matches with the real ground surfaces. The generated surface patterns result from the kinematics of the grinding process combined with small runout of the grinding wheel or/and small deviations in grain protrusion heights as well as speed ratio deviations between workpiece and grinding wheel while grinding. The kinematics of the grinding process have significant influence on the pattern formation. To improve the surface quality it is necessary to avoid the generation of these surface patterns. The developed simulation turned out to be a useful tool to improve the interaction of grinding wheel and workpiece before machining. The results show that high requirements in the tool adjustments, balancing, parameter settings and control of the machine tool (e.g. closed-loop speed control for the spindle systems), must be demanded.

4 ACKNOWLEDGMENTS

The authors express their sincere thanks to the DFG for funding this project, which is part of the transregional collaborative research center SFB/TR4 “Process chains for the replication of complex optical components”.

5 REFERENCES

[1] Fawcett, S.-C., Dow, T.-A., 1991, Development of a model for precision contour grinding of brittle materials, Precision Engineering, 13/4:270-276.

[2] Byrne, G., Dornfeld, D., Denkena, B., 2003, Advanced Cutting Technology, Annals of the CIRP, 52/2:1-25.

[3] Tönshoff, H.K., Peters, J., Inasaki, I. Paul, T., 1992, Modeling and Simulation of Grinding Processes, Annals of the CIRP, 41/2:677-688.

[4] Chen, X., Rowe, W.-B., 1996, Analysis and Simulation of Grinding Process Part I: Generation of the Grinding Wheel Surface, International Journal of Machine Tools and Manufacture, 36:871-882.

[5] Li, Y., Gracewski, S.M. Funkenbusch, P.D., Ruckman, J., 2002, Analysis of chatter in contour grinding of optical materials, International Journal of Machine Tools & Manufacture, 42, 1095-1103.

[6] Bifano, T.G., Dow, T.A., Scattergood, R.O., 1991, Ductile-regime grinding: a new technology for machining brittle materials, Journal of Engineering for Industry, 113 (2), 184.

[7] Inasaki, I., Karpuschewski, B., Lee, H.-S., 2001, Grinding Chatter – Origin and Suppression, Annals of the CIRP, 50/2:1-20.

[8] Salisbury, E.J. et al., 2001, A Three-Dimensional Model for the Surface Texture in Surface Grinding, Part 1: Surface Generation Model, Journal of Manufacturing Science and Engineering, 123, 576-581.

[9] Yang, F., Zhang, B., Wang, J., Zhu, Z., Monahan, R., 2001, The Effect of Grinding Machine Stiffness on Surface Integrity of Silicon Nitride, Journal of Manufacturing Science and Engineering, 123:591-600.

[10] Komanduri, R., Lucca, D.A., Tani, Y., 1997, Technological Advances in Fine Abrasive Processes, Annals of the CIRP, 46/2:545-596.